Journal of Inflammation Research

Dovepress
Taylor & Francis Group

Open Access Full Text Article

ORIGINAL RESEARCH

Upadacitinib Attenuates Lipopolysaccharide- and Cecal Ligation and Puncture-Induced Inflammatory Responses by Inhibiting NF-κB and Its Downstream Cytokines

Qi Yao[1,*], Xueting Yang[1,*], Hongli Yan[2,*], Yang Wang[3], Yanlin Ma[1], Ning Xu[4]

[1]Department of Pharmacy, The First People's Hospital of Yunnan Province, The Affiliated Hospital of Kunming University of Science & Technology, Kunming, 650032, People's Republic of China; [2]Department of Pharmaceutics, Yunnan University of Traditional Chinese Medicine, Kunming, 650500, People's Republic of China; [3]Department of General Surgery, The First People's Hospital of Yunnan Province, The Affiliated Hospital of Kunming University of Science and Technology, Kunming, 650032, People's Republic of China; [4]Department of Clinical Laboratory, The First People's Hospital of Yunnan Province, The Affiliated Hospital of Kunming University of Science and Technology, Kunming, 650032, People's Republic of China

*These authors contributed equally to this work

Correspondence: Qi Yao; Ning Xu, Department of Pharmacy, The First People's Hospital of Yunnan Province, Kunming, Yunnan, People's Republic of China, Tel/Fax +86-871-63645556, Email yjj_519@126.com; xuning_0629@yeah.net

Background: Upadacitinib (UPA) is a selective tyrosine kinase 1 (JAK-1) inhibitor, which has been applied to treat atopic dermatitis, psoriatic arthritis, and ulcerative colitis in clinic. Whether it can treat sepsis remains unclear. Here, we investigate the effect of UPA on lipopolysaccharide (LPS)- and cecal ligation and puncture (CLP)-induced inflammatory responses in vitro and in vivo.

Methods: In vitro, LPS-treated RAW264.7 cell line, LPS-treated TLR4 knock-out ($TLR4^{-/-}$) RAW264.7 cell line, and LPS-treated NLRP3 knock-out ($NLRP3^{-/-}$) RAW264.7 cell line were used. In vivo, CLP-treated mice and CLP-treated $TLR4^{-/-}$ mice were used. Proteomics was used to screen inflammation-related differential proteins in RAW264.7 cells after treatments. After that, Western blotting was used to investigate the potential mechanism.

Results: In vitro, UPA significantly inhibited TLR4/NF-κB and JAK/STAT pathway in the LPS-treated RAW264.7 cells. In addition, UPA reduced protein expressions of NF-κB and its downstream inflammatory cytokines such as TNF-α, IL-1β in the LPS-treated $TLR4^{-/-}$ RAW264.7 cells. In vivo, UPA markedly protected the sepsis mice, decreased intestinal injuries, reduced bacterial load, and downregulated the TLR4/NF-κB and JAK/STAT pathways-related proteins in macrophages isolated from peritoneal lavage fluids (PLFs) of the sepsis mice. In fact, UPA still exerted the protective effect in the CLP-treated $TLR4^{-/-}$ mice. The proteomics revealed that NOD-like receptor (NLR) signaling was one of the most significantly affected pathways between the LPS-treated and UPA-treated. Although UPA significantly reduced NLRP3 and IL-1β protein expressions in the LPS-treated RAW264.7 cells, its anti-inflammatory effect was not significantly abolished in the LPS-treated $NLRP3^{-/-}$ RAW264.7 cells.

Conclusion: Taken together, UPA inhibits the LPS- and CLP-induced inflammatory responses in vitro and in vivo, which is associated with the inhibition of NF-κB and its downstream cytokines.

Keywords: upadacitinib, TLR4, NLRP3, RAW264.7 cells, mice, proteomics

Introduction

In clinic, gram-negative bacteria-induced severe infection often leads to systemic inflammatory response syndrome (SIRS), which ultimately develops into sepsis, septic shock, and even multiple organ dysfunction syndrome (MODS). The mortality rate of sepsis remains high, with a mortality rate of over 50%, which proposes a serious threat to patients' lives.[1]

Received: 21 April 2025
Accepted: 30 August 2025
Published: 10 September 2025

Graphical Abstract

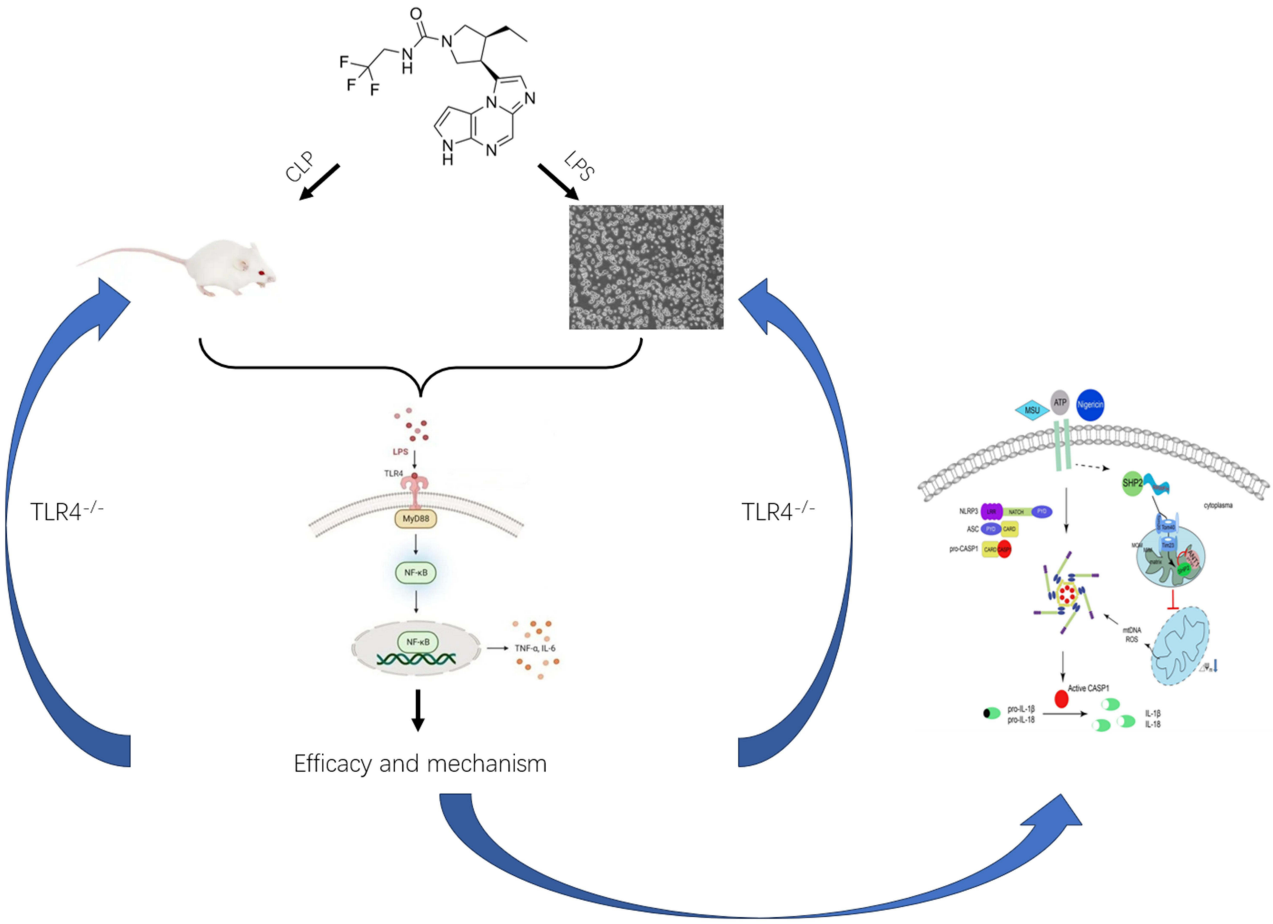

It has been widely accepted that toll-like receptor 4 (TLR4) plays a crucial role in the process of sepsis[2] (Wang et al, 2021). LPS binds to membranous TLR4 to activate MyD88 and downstream NF-κB, which releases a large number of proinflammatory cytokines such as TNF-α, IL-6, IL-1β which are crucial in initiation and development of sepsis.[3] Additionally, a recent study has reported that deletion of TLR4 significantly increases survival rate, improves tissue injuries, and reduces proinflammatory mediates' levels of sepsis mice.[4] So, it is promising to treat sepsis by targeting TLR4.[5,6]

Now, researchers have developed TLR4 inhibitors such as E5564 (eritoran)[4] and TAK-242,[7] TLR9 agonist IMO 2125,[8] and TLR7 agonist Imiquimod (Aldara).[9] However, these target reagents are still in the preclinical or clinical trial stage yet.

Upadacitinib (UPA) (Figure 1a), a selective tyrosine kinase 1 (JAK-1) inhibitor, has been developed by the Abbvie company. It has been used to treat atopic dermatitis,[10] rheumatoid arthritis,[11] psoriatic arthritis,[12] and ulcerative colitis.[13]

The JAK/STAT pathway is a core pathway for cytokines such as interferon, interleukins, which is involved in the regulation of excessive inflammatory response and immune suppression in sepsis.[14] Further, this pathway regulates macrophage polarization (M1/M2 type) by activating STAT proteins, affecting organ dysfunction including sepsis-related lung injury.[15] A recent study has confirmed that tofacitinib significantly inhibited the expressions of inflammatory factors and improved lung histopathological injury in septic rats via inhibiting JAK-STAT/NF-κB pathway.[16] Previously, a study has revealed that UPA suppresses M1 macrophage infiltration in alkali-injured corneas by decreasing mRNA levels of

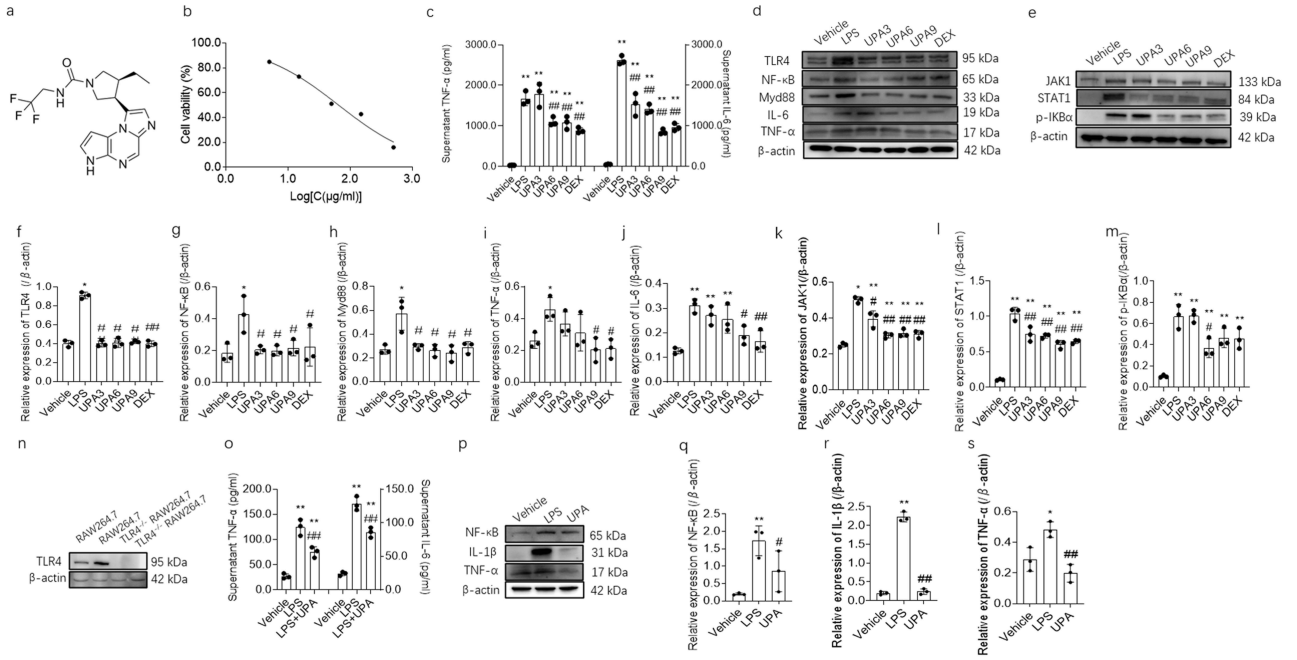

Figure 1 UPA inhibits LPS-induced inflammatory responses in vitro. (**a**) Chemical structure of UPA; (**b**) Cytotoxicity assay of UPA for RAW264.7 cells ($\bar{x} \pm s$, n = 3). The IC_{50} value of UPA for RAW264.7 cells was conducted in accordance with instructions of the CCK-8 kits; (**c**) UPA downregulates supernatant TNF-α and IL-6 released from LPS-treated RAW264.7 cells ($\bar{x} \pm s$, n = 3). $^{**}p < 0.01$ vs Vehicle, $^{\#}p < 0.05$, $^{\#\#}p < 0.01$ vs LPS. The cell supernatants were collected at 4 h after the LPS stimulation. Next, the supernatant TNF-α and IL-6 were detected by using ELISA kits. The OD values of the solutions were determined by using a microplate reader at 450 nm; (**d–m**) UPA inhibits expressions of TLR4/ NF-κB and JAK1/STAT1 pathways-related proteins in LPS-treated RAW264.7 cells ($\bar{x} \pm s$, n = 3). $^{**}p < 0.01$ vs Vehicle, $^{\#}p < 0.05$, $^{\#\#}p < 0.01$ vs LPS. The collected cell precipitates were lysed and then ultrasonicated on ice. Centrifuged at 12,000 × g to harvest the supernatants. Next, the total proteins were separated, semi-dry transferred on PVDF membranes. After blocked with 5% fat-free milk, primary anti- antibodies and secondary antibodies were added in sequential orders. Finally, the membranes were visualized by ECL detection on an imaging system. (**n**) Western blotting assay of TLR4 protein in RAW264.7 cells and TLR4$^{-/-}$ RAW264.7 cells. (**o**) UPA decreases supernatant TNF-α and IL-6 released from LPS-treated TLR4$^{-/-}$ RAW264.7 cells ($\bar{x} \pm s$, n = 3). $^{**}p < 0.01$ vs Vehicle, $^{\#\#}p < 0.01$ vs LPS. The supernatant TNF-α and IL-6 were measured by the ELISA method; (**p–s**) UPA reduces NF-κB, TNF-α, and IL-1β protein expressions in LPS-treated TLR4$^{-/-}$ RAW264.7 cells ($\bar{x} \pm s$, n = 3). $^{*}p < 0.05$, $^{**}p < 0.01$ vs Vehicle, $^{\#}p < 0.05$, $^{\#\#}p < 0.01$ vs LPS. The Western blotting assay were conducted to measure NF-κB, TNF-α, and IL-1β protein proteins.

inflammatory mediators such as TNF-α, IL-6, and IL-1β. Moreover, UPA in vitro inhibits M1 macrophage polarization by suppressing IFN-γ/LPS-induced STAT1 activation in a dose-dependent manner.[17] Up to now, few studies have reported the anti-inflammatory effects of UPA in the sepsis-related models. In view of this, it is necessary to clarify the efficacy and mechanism of this JAK inhibitor in sepsis and its related organ damage, which will be beneficial to extend its clinical indications.

Proteomics is a key technique to elucidate action mechanisms of drugs by systematically analyzing changes in protein expression, modification, and interaction networks.[18] The analysis of drug action mechanisms mainly includes functional proteomics analysis and protein interaction network analysis.[19]

In the present study, the anti-inflammatory efficacy of UPA was investigated in the LPS-treated RAW264.7 cells and CLP-treated mice. After that, the mechanisms in vitro and in vivo were investigated in TLR4$^{-/-}$ RAW264.7 cells and TLR4$^{-/-}$ mice. Moreover, proteomics combined with experiment validation was conducted to explore its mechanism more accurately. This study will provide a promising medication for sepsis and its related complications.

Materials and Methods

Cell Lines and Experimental Animals

The RAW264.7 cell line was purchased from Procell Life Science & Technology Co., Ltd. (Wuhan, China). A total of 92 male specific pathogen free (SPF) institute of cancer research (ICR) mice (20–22 g) was obtained from Huabukang Biotechnology Co., Ltd. (Beijing, China). The TLR4$^{-/-}$ RAW264.7 cell line (Catalog No.: SY-KO-00286, Lot No.: 20240408R31), NLRP3$^{-/-}$ RAW264.7 line (Catalog No.: SY-KO-00441, Lot No.: 20240725R31) were provided by

Cyagen Biosciences Inc. (Taicang, Jiangsu, China). Also, three pairs of TLR4$^{-/-}$ mice (Genotyping: C57BL/6NCya-*Tlr4*^{em1}/Cya) (Batch No. S-KO-05468) (gender ratio of 1:1) were provided by Cyagen Biosciences Inc. (Taicang, Jiangsu, China) (18–22 g). The male and female mice were housed with a ratio of 1:1, and the animals were housed separately after 15 days of the enclosure. After 10 days of the separation, the male and female mice were housed again if no obvious signs of pregnancy. Once pregnancy, the female and male animals must be separated for 7 days after the birth. After that, the newborn mice were validated by detecting TLR4 mRNA in the tails using reverse transcription-polymerase chain reaction (RT-PCR). Further, the TLR4 protein in the intestines was detected by Western blotting. All the mice were raised in a SPF experiment animal room at room temperature (20°C) with a 12-hour light–dark cycle. The animal experiment protocol was approved by the Ethics Committee of Animal Experiments of Yunnan University of Traditional Chinese Medicine, and the ethnic batch number was R-062024G148. This study was performed according to the NIH Guide for the Care and Use of Laboratory Animals.

Main Reagents

UPA [RINVOQ®(15mg)] (Batch No. 1172159) was purchased from AbbVie Ireland NL B.V. (Manorhamilton Road, Sligo, Ireland). Dexamethasone (DEX) sodium phosphate injection (Batch No. 36428) was provided by Huazhong Pharmaceutical Co., Ltd. (Xiangyang, Hubei, China). The TLR4 (Batch No. J0821), and MyD88 (Batch No. F2218) primary antibodies were obtained from Santa Cruz Biotechnology (Shanghai, China). The NF-κB (Batch No. ab16502) and NLRP3 (Batch No. ab263899) primary antibody was purchased from Abcam Inc. (Shanghai, China). The p-iκBα (Batch No. 4812S) primary antibody was obtained from Cell Signaling Technology Inc. (Shanghai, China). The TNF-α (Batch No. 10026111), IL-6 (Batch No. 10022178), IL-1β (Batch No. 00139659), JAK1 (Batch No. 10004856), STAT1 (Batch No. 00120876), NF-κB p65 (Batch No. KHC0634), Bmi1 (Batch No. KHC0296) and Lgr5 (Batch No. 30007-1-AP) primary antibodies for immunohistochemistry assays were obtained from Proteintech Group Inc. The secondary anti-mouse antibody (Batch No. 7076S) and the secondary anti-rabbit antibody (Batch No. 7074S) were purchased from Cell Signaling Technology (Shanghai, China). The mouse TNF-α (Batch No. 1217202) and IL-6 (Batch No. 1210602) ELISA kits were obtained from Dakewe Biotech Co., Ltd. (Shenzhen, China).

Cell Viability Assay

The RAW264.7 cells (10^5/well) at passage 3–5 were cultured in Dulbecco's modification of Eagle's medium (DMEM) containing 1% penicillin-streptomycin and 10% fetal bovine serum. After the cells were cultured in a 96-well plate (10^4/well) for 12 h, the medium was replaced with serum-free medium. Respectively, 1 μL UPA with various concentrations were added to co-culture for another 24 h. After that, 10 μL cell counting kit-8 (CCK-8) solution (Solarbio Life Sciences, Beijing, China) was added and co-cultured for another 2 h. Finally, the optical density (OD) values of the solutions were measured at 450 nm by using a MutiskanGo microplate reader (Thermo Scientific, Massachusetts, USA).

Treatments of RAW264.7 Cells and TLR4$^{-/-}$ RAW264.7 Cells for Cytokine Assays

For the RAW264.7, the cells (10^5/well) were seeded in a 6-well plate and cultured for 12 h. Then, the cells were respectively treated with various concentrations of UPA (3, 6, and 9 μg/mL) and DEX (4 μg/mL). For the TLR4$^{-/-}$ RAW264.7, UPA (9 μg/mL) was used to treat the cells. Subsequently, LPS was added to reach a final concentration of 1 μg/mL. Meanwhile, the vehicle and LPS treatment were set parallelly. Four hours after the LPS treatment, the cell supernatants and precipitates were collected for ELISA and Western blotting assays, respectively.

Western Blotting Assay

The collected RAW264.7 or TLR4$^{-/-}$ RAW264.7 cell precipitates were lysed by boiling 1 × loading buffer (Beyotime Biotech, Haimen, China) and then ultrasonicated on ice for 30 seconds by using a SCIENTZ-IID ultrasonic Homogenizer (Xinzhi Biotech Co. Ltd, Ningbo, China). Centrifuged at 12,000 × *g* for 5 min at 4°C to harvest the supernatants. Next, the total proteins were separated using 10% SDS-PAGE and subsequently transferred via semi-dry blotting. The membranes were blocked with 5% fat-free milk dissolved in tris buffered saline containing Tween20 (TBST).

Respectively, co-cultured the membranes with anti-TLR4 (1:1000), -MyD88 (1:1000), -NF-κB (1:2000), p-iκBα (1:1000), -JAK1 (1:1000), -STAT1 (1:1000), -NLRP3 (1:1000), -TNF-α (1:1000), -IL-6 (1:1000), and -IL-1β (1:1000) antibodies for 2 h at room temperature to assay the proteins in the RAW264.7 cells. Correspondingly, respectively added anti-NF-κB (1:2000), -TNF-α (1:1000), and -IL-1β (1:1000) antibodies to co-culture with the membranes to detect the proteins in the $TLR4^{-/-}$ RAW264.7 cells.

After washed the membranes three times, added secondary anti-mouse antibody (1:5000) or anti-rabbit antibody (1:5000) respectively to co-culture for another 1 h. The membranes were visualized by enhanced chemiluminescence (ECL) detection on a ChemiDocTM Imaging System (BIO-RAD, Hercules, CA, USA).

CLP-Induced Sepsis Models in ICR Mice and $TLR4^{-/-}$ Mice

A total of 60 ICR mice were randomly divided into a sham group, a model group, a DEX group (4 mg/kg), and two UPA groups (3 and 6 mg/kg, i.g, 12 animals in each group) (UPA dissolved in 5% CMC-Na) using a random number table method. The mice received various treatments once a day for continuous 5 days. Four hours after the last treatments, the animals received the CLP surgeries except for the sham ones after intraperitoneal injections of 0.3% pentobarbital (50 mg/kg). Briefly, a midline abdominal incision (1–1.5 cm) was made in an anesthetized mouse, and the cecum was exposed by sequential dissection. The cecum was ligated at approximately the midpoint between the distal cecum and ileocecal valve. An 18-gauge needle was used to puncture the ligated end, and a small amount of intestinal content was gently extruded out. The peritoneum and skin were subsequently sutured, followed by an immediate subcutaneous injection of physiological saline (50 mg/kg).

Six hours post the surgeries, the peripheral blood samples were collected by sequential bleeds and then centrifuged to harvest the sera for the ELISA assay (n = 6). Animal mortality was recorded daily for 7 days. At the end of the experiments, the survival curves of groups were plotted to assess the anti-infection of UPA. The small intestines were immediately collected for the pathology when the animals were dead or sacrificed by cervical dislocation.

In addition, 30 ICR mice were randomly divided into 5 groups including a sham group, a CLP group, two UPA groups (3 and 6 mg/kg), and a DEX group (4 mg/kg) (6 in each group) using a random number table method. The mice were treated described as before. Four hours after the last treatments, the animals received the CLP surgeries except for the sham ones. Six hours after the surgeries, all the animals were sacrificed by cervical dislocation. The dead mice were soaked in 75% ethanol for 5 min. An aliquot (5 mL) of PBS was injected into the abdominal cavity using a sterile syringe. Under aseptic conditions, the abdominal skin was incised, and a sterile Pasteur pipette was introduced through the opening to access the peritoneal cavity. Rinsed the peritoneal lavage fluids (PLFs) gently twice and collected for subsequent analysis. The whole process was performed in a biosafety cabinet. Then, 100 μL of diluted PLFs (1: 1×10^6) were uniformly spread onto sterile columbia blood agar plates, and cultured in an incubator at 37°C for 24 h. The colony forming units (CFUs) were counted and the differences among groups were compared.

The remaining PLFs were centrifuged at 1000 rpm/min for 10 min at room temperature. After that, the precipitates were resuspended and seeded in RPMI 1640 culture medium. Two to three hours after the inoculation, the non-adherent cells were discarded. Subsequently, the adherent cells were digested by 0.5% Trypsin-EDTA and centrifuged at 1000 rpm/min for 10 min to collect the precipitates for Western blotting analysis.

After the validations, 18 $TLR4^{-/-}$ mice were randomly separated into a vehicle group, a CLP group, and a UPA group (6 mg/kg, i.g) (6 in each group). The mice received various treatments for continuous 5 days and once a day. Four hours after the last treatments, the animals were intraperitoneally injected with 0.3% pentobarbital (50 mg/kg). Then the CLP surgeries were performed in the animals except for the sham ones. The peripheral blood collections were conducted as well as the ICR mice. The survival of all the animals was recorded daily for 7 days post the interventions. Survival curves were plotted, and differences among groups were assayed using Kaplan–Meier analysis. The small intestinal tissues were collected for pathology, immunohistochemistry, and immunofluorescence assays.

Intestinal Pathology of CLP-Treated ICR Mice or CLP-Treated $TLR4^{-/-}$ Mice

The collected small intestines were fixed in 4% paraformaldehyde for 24 h, and then dehydrated and embedded in paraffins. Next, the paraffin samples were cut into 2 μm-thick sections consecutively followed by staining with hematoxylin and eosin (H&E). The pathological changes especially edema, inflammation, and hemorrhage were

observed and imaged by a DM750 microscope (Leica, Weztlar, Germany). The pathological scores were assessed in accordance with Chiu's grading.[20] The pathological scoring was performed by two independent investigators, and any discrepancy was resolved by a consensus.

Western Blotting Assays of Intestinal TLR4, NF-κB, MyD88, Bmi1, and Lgr5 Proteins

The TLR4, NF-κB, and MyD88 proteins in the small intestines of the CLP-treated mice, and NF-κB, Bmi1, and Lgr5 proteins in the small intestines of the CLP-treated $TLR4^{-/-}$ mice were detected by Western blotting.

Immunohistochemistry of NF-κB in Small Intestines

The collected intestines were treated as before. The 2-μm-thick sections were dewaxed with xylene solutions and then hydrated with multi-gradient ethanol solutions.

After antigen repairing, the sections were placed in 0.3% PBST solution for 20 min and then washed with PBS three times. An immunohistochemistry assay kit was used to detect NF-κB expression in the small intestines.

Endogenous peroxidase was added to the sections in a wet box, incubated at room temperature for 10 min, rinsed and then blocked with 5% sheep serum for 30 min at room temperature. After that, the NF-κB (1:100) primary antibody was added to co-incubate for 1 h at 37°C and then washed with PBS. Subsequently, the secondary antibody was added to co-incubate for 20 min at room temperature and then rinsed. Finally, 3,3′-diaminobenzidine (DAB) was added and incubated for 3 min to terminate the reaction. Re-staining was performed using H&E staining for 30–60s. The positive granules labelled with brownish yellow were observed under an inverted microscope.

Immunofluorescence Assays of Bmi1 and Lgr5 in Small Intestines

After deparaffinization, the antigen repairing was conducted for the paraffin sections. Added 5% BSA to block for 30 min, and then added anti-mouse Bmi1 (1:50) or anti-mouse Lgr5 (1:50) antibody to co-incubate overnight at 4°C. Washed the slices with PBS three times. After that, added fluorescence-labelled secondary antibody and co-incubated in the dark at 37°C for 1 h. Washed three times, and then added anti-fluorescence quencher containing 4′,6-diamidino-2-phenylindole (DAPI) (Thermo Fisher Scientific, Waltham, MA, United States) for sealing. Finally, imaged under a TE2000-U inverted fluorescence microscope (Nikon, Tokyo, Japan).

Proteomics Assays of Differential Proteins and Pathways in RAW264.7 Cells

The RAW264.7 cells at passages 3–5 were treated with UPA (9 μg/mL) followed by LPS treatment (1 μg/mL). A vehicle and a LPS treatment were set as parallel controls. Four hours after the treatments, the supernatants were removed and the cellular precipitates were collected.

The cells were lysed for 5 min using ice-cold lysis buffer containing 8 M urea, 1 mM PMSF and 2 mM EDTA. The lysates were then centrifuged at 15,000 × g for 10 minutes at 4°C to harvest the supernatants. Total protein concentration was quantified using the BCA method. After enzymatic digestion, the digested peptides were desalted using C18 solid-phase extraction columns, concentrated by vacuum centrifugation, and reconstituted by 0.1% (v/v) formic acid.

Chromatographic separation was performed on a NanoElute UHPLC system (Bruker) using an IonOpticks Aurora C18 column (1.6 μm, 25 cm × 75 μm) maintained at 50°C. The MS analysis was conducted by a timsTOF Pro mass spectrometer (Bruker) in data-dependent acquisition mode.

The data-independent acquisition mass spectrometry (DIA-MS) were processed using DIA neural network (DIA-NN) software (version 1.8.1) in Library-free mode. Protein quantification was performed by the MaxLFQ algorithm integrated in DIA-NN. After the quantification, the intensity values of each protein across different samples were extracted from the search results. These values were subsequently normalized through zero-centered scaling to obtain relative protein quantification values for comparative analysis.

Western Blotting of Differential Proteins in LPS-Treated RAW264.7 Cells and Validations in LPS-Treated NLRP3$^{-/-}$ RAW264.7 Cells

The RAW264.7 cells were respectively treated with various concentrations of UPA (3–9 μg/mL). After that, added LPS (1 μg/mL) to treat the cells for 4 h. Meanwhile, the vehicle was set parallelly. The cell precipitates were collected for Western blotting assays of NLRP3 and IL-1β.

Further, the NLRP3$^{-/-}$ RAW264.7 cell line was used to explore the role of NLRP3 in the anti-inflammatory effect of UPA in vitro. Briefly, the cells at passage 3–5 were respectively treated with vehicle, LPS (1 μg/mL), and LPS (1 μg/mL) plus UPA (9 μg/mL). Four hours post the treatments, the precipitates were collected. Then the NF-κB, TNF-α, and IL-1β proteins were measured by Western blotting.

Data Presentation and Statistics

The data were expressed as mean ± SEM. One-way analysis of variance (ANOVA) was used to compare significance among the groups. GraphPad Prism (v.8.3.0, San Diego, CA, USA) was used for statistical analysis. *T*-test was used comparison between two groups. Kaplan–Meier and Log rank tests were used for survival analysis. The sample size was pre-calculated for power or effect size. In addition, the data distribution (normality) was assessed before application of ANOVA. Tukey's post hoc test was used to compare differences among groups if the data were not normally distributed. The testing level is set at $p < 0.05$.

Results

UPA Inhibits LPS-Induced Inflammatory Responses in RAW264.7 Cells

UPA inhibited the cellular growth in a dose-dependent manner, which displayed some cytotoxicity for the RAW264.7 cells. The IC_{50} value of this compound was appropriately 65.32 μg/mL using the Bliss method (Figure 1b).

Compared with the vehicle, LPS treatment significantly increased supernatant TNF-α and IL-6 levels, respectively. UPA at 6 and 9 μg/mL and DEX at 4 μg/mL markedly reduced the increased supernatant TNF-α and IL-6 levels compared to the LPS treatment alone (TNF-α: F = 59.51, $p = 0.0099$; IL-6: F = 153.6, $p = 0.0009$) (Figure 1c).

In addition, the LPS treatment significantly increased the TLR4/NF-κB and JAK1/STAT1 pathways-related protein expressions, while UPA at 3–9 μg/mL and DEX at 4 μg/mL remarkably reduced the increased expressions of these protein including TLR4 (F = 109.2, $p < 0.0001$), Myd88 (F = 9.075, $p = 0.0009$), NF-κB (F = 12.16, $p = 0.0321$), p-iκBα (F = 19.22, $p < 0.0001$), JAK1 (F = 39.84, $p < 0.0001$), STAT1 (F = 70.58, $p < 0.0001$), TNF-α (F = 4.774, $p = 0.0124$), and IL-6 (F = 9.866, $p = 0.0006$) (Figure 1d–m).

UPA Exerts Anti-Inflammatory Effect in LPS-Treated TLR4$^{-/-}$ RAW264.7 Cells

The Western blotting showed that the TLR4 protein was not detected in the TLR4$^{-/-}$ RAW264.7 cells compared to the RAW264.7 cells (Figure 1n).

The supernatant TNF-α and IL-6 levels of the LPS-treated TLR4$^{-/-}$ RAW264.7 cells were remarkably elevated compared to the vehicle. Further, the supernatant cytokines levels were far lower than those of the LPS-treated RAW264.7 cells. Compared with the LPS, UPA (9 μg/mL) markedly reduced the increased supernatant TNF-α and IL-6 levels (TNF-α: F = 55.00, $p = 0.006$; IL-6: F = 99.86, $p = 0.0065$) (Figure 1o). Additionally, UPA and DEX significantly downregulated cellular NF-κB (F = 10.06, $p = 0.0121$), IL-1β (F = 488.1, $p < 0.0001$), and TNF-α (F = 15.80, $p = 0.0041$) compared to the LPS (Figure 1p–s).

UPA Increases Survival Rate and Reduces Serum TNF-α and IL-6 Levels of CLP-Treated Mice

After the CLP surgeries, the major animals died from 24 h to 48 h, and all the animals in the CLP group died within 72 hours (Figure 2a). The UPA (6 mg/kg) and DEX (4 mg/kg) significantly elevated the animal survival rate compared to the model after Log-rank (Mantel-Cox) test (Chi square = 32.99, $p < 0.0001$) (Figure 2a). Further, the serum TNF-α and

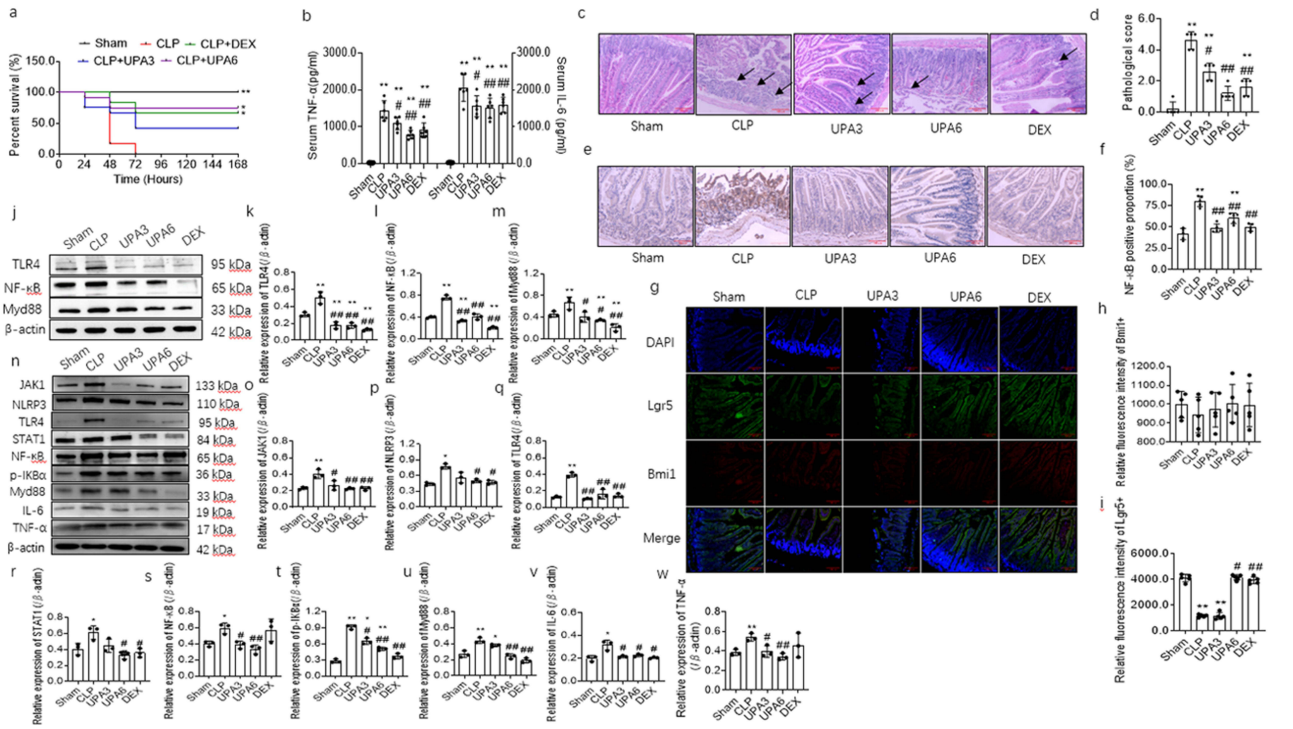

Figure 2 UPA protects CLP-induced sepsis mice. (**a**) Animal survival of among groups (Kaplan-Meier). *p < 0.05, **p < 0.01 vs CLP. After the CLP surgeries, the animal survival of each group was observed and recorded daily for 7 days. At 168 h, the survival curves were plotted and the differences among groups were compared; (**b**) Serum TNF-α and IL-6 assays of the sepsis mice ($\bar{x} \pm s$, n = 6). **p < 0.01 vs Vehicle, $^{\#}p$ < 0.05, $^{\#\#}p$ < 0.01 vs CLP. The peripheral blood was collected 6 h after the CLP surgeries. Next, the sera were isolated, and the serum TNF-α and IL-6 levels were detected by using ELISA kits in accordance with the instructions; (**c** and **d**) Pathology and score of small intestines of sepsis mice in groups ($\bar{x} \pm s$, n = 5) (Bar = 50 μm). **p < 0.01 vs Sham, $^{\#}p$ < 0.05, $^{\#\#}p$ < 0.01 vs CLP. The collected small intestines were fixed in 4% paraformaldehyde and dehydrated. Next, the paraffin sections were then stained with H&E. The pathological changes especially edema, inflammation, and hemorrhage were observed. Chiu's grading was used to assess the pathological scores for the small intestines; (**e** and **f**) Immunohistochemistry assay of NF-κB protein in small intestines of sepsis mice in groups ($\bar{x} \pm s$, n = 5) (Bar = 50 μm). **p < 0.01 vs Sham, $^{\#\#}p$ < 0.01 vs CLP. The embedded small intestine paraffins were dewaxed and hydrated. After antigen repairing, an immunohistochemistry assay kit was used to assay NF-κB expression in the small intestines; (**g–i**) Immunofluorescence staining assays of Bmi1 and Lgr5 in small intestines of sepsis mice ($\bar{x} \pm s$, n = 5) (Bar = 50 μm). **p < 0.01 vs Vehicle, $^{\#}p$ < 0.05, $^{\#\#}p$ < 0.01 vs CLP. After deparaffinization, the antigen repairing was conducted. Added Bmi1 or Lgr5 antibody to co-incubate with the sections overnight. Then added fluorescence-labelled secondary antibody and co-incubated in the dark. Imaged under an inverted fluorescence microscope; (**j–m**) Western blotting assays of TLR4, MyD88, and NF-κB proteins in small intestines of sepsis mice ($\bar{x} \pm s$, n = 3). **p < 0.01 vs Sham, $^{\#}p$ < 0.05, $^{\#\#}p$ < 0.01 vs CLP. The collected intestines were lysed and then ultrasonicated. Centrifuged to harvest the supernatants. After that, the Western blotting was performed to determine TLR4, MyD88, and NF-κB protein expressions; (**n–w**) Western blotting assays of inflammation-related proteins in PLFs-isolated macrophages of sepsis mice ($\bar{x} \pm s$, n = 3). **p < 0.01 vs Sham, $^{\#}p$ < 0.05, $^{\#\#}p$ < 0.01 vs CLP. The macrophages were isolated from the PLFs. After that, the Western blotting was performed to assay the inflammation-related proteins.

IL-6 levels in the UPA groups (3 and 6 mg/kg) and DEX (4 mg/kg) group were respectively lower than those in the CLP group (TNF-α: F = 53.19, p < 0.0001; IL-6: F = 54.94, p < 0.0001) (Figure 2b).

UPA Attenuates Intestinal Injuries of CLP-Treated Mice

The CLP surgery caused inflammatory cell infiltration, intestinal edema, and loss of intestinal epithelial integrity. Meanwhile, irregular arrangement of the intestinal glands, swollen epithelial cells, and loose and lightly stained cytoplasm could be observed (shown by arrows) (Figure 2c). The high-dose UPA significantly restored intestinal epithelial integrity, reduced intestinal edema and inflammatory cell infiltration. In addition, UPA significantly reduced the intestinal pathological score compared to the CLP (F = 53.62, p < 0.0001) (Figure 2d).

UPA Downregulates Intestinal NF-κB Expression in CLP-Treated Mice

The immunohistochemistry showed that the expression of NF-κB protein (brown granules) was higher in the CLP group than that in the sham group. Compared with the CLP, the high-dose UPA and DEX significantly reduced the NF-κB expression in the small intestines (F = 34.60, p < 0.0001) (Figure 2e and f).

UPA Upregulates Intestinal Lgr5 Expression in CLP-Treated Mice

The CLP markedly downregulated the expression of proliferation-related protein Lgr5 in the small intestines compared to the sham. UPA treatment had no significant effect on the positive expression of Bmi1 ($F = 0.3444$, $p = 0.8448$) (Figure 2h). Compared with the CLP, UPA and DEX remarkably upregulated the intestinal Lgr5 expression ($F = 191.1$, $p < 0.0001$) (Figure 2g and i).

UPA Reduces Intestinal TLR4 Pathway-Related Protein Expressions in CLP-Treated Mice

The expressions of TLR4, NF-κB, and Myd88 proteins were higher in the CLP group than those in the sham group. UPA and DEX significantly reduced the increased expressions of these three proteins in the small intestines compared to the CLP (TLR4: $F = 43.43$, $p = 0.0081$; NF-κB: $F = 148.3$, $p = 0.0029$; Myd88: $F = 11.15$, $p = 0.0404$) (Figure 2j–m).

UPA Reduces Bacterial Load in PLFs of CLP-Treated Mice

In the CLP group, the bacterial CFUs in the PLFs were significantly higher than those in the sham group. It revealed that UPA and DEX markedly reduced the bacterial loads compared to the CLP, respectively ($F > 886.8$, $p < 0.0001$) (Table 1).

UPA Reduces Inflammation-Related Protein Expressions in Isolated Macrophages

The Western blotting showed that inflammation-related protein expressions were significantly higher in the CLP group than those in the sham group, respectively. It showed that UPA remarkably reduced the increased expressions of these proteins including TLR4 ($F = 43.67$, $p < 0.0001$), Myd88 ($F = 31.29$, $p < 0.0001$), NF-κB ($F = 6.959$, $p = 0.0060$), p-iκBα ($F = 99.41$, $p < 0.0001$), JAK1 ($F = 12.40$, $p = 0.0007$), STAT1 ($F = 7.327$, $p = 0.0050$), NLRP3 ($F = 16.95$, $p = 0.0002$), TNF-α ($F = 3.895$, $p = 0.0369$), and IL-6 ($F = 12.11$, $p = 0.0008$), which was some consistent with the Western blotting results in vitro (Figure 2n–w).

UPA Increases Animal Survival and Reduces Serum TNF-α and IL-6 Levels of CLP-Treated TLR4$^{-/-}$ Mice

Compared with the wild type (WT) mice, the sham led to almost no TLR4 expression in the intestines of the TLR4$^{-/-}$ mice. In addition, the CLP caused a very small amount of TLR4 expression in the intestines of this gene knockout mice (Figure 3a).

It showed that some of the CLP-treated TLR4$^{-/-}$ mice died within 72 hours (Figure 3b), which was some different from the CLP-treated ICR mice. Also, UPA (6 mg/kg) still significantly increased the survival rate of the CLP-treated TLR4$^{-/-}$ mice (Chi square = 9.404, $p = 0.0091$) (Figure 3b). Further, the serum TNF-α and IL-6 levels were lower in the UPA group than those in the CLP group (TNF-α: $F = 23.91$, $p < 0.0001$; IL-6: $F = 54.89$, $p < 0.0001$) (Figure 3c).

Table 1 Bacterial Load in PLFs After Treatments ($\bar{x} \pm s$, n = 3)

Group	Dose (mg/kg)	CFU
Sham	–	$31.7 \pm 3.5^{\#\#}$
CLP	–	>200.0
Low-dose UPA	3	>200.0
High-dose UPA6	6	$34.7 \pm 9.1^{\#\#}$
DEX	4	$29.0 \pm 7.0^{\#\#}$

Notes: $^{\#\#}p < 0.01$ vs CLP. The 100 μL diluted PLFs were spreaded onto sterile columbia blood agar plates. Then cultured in an incubator at 37°C for 24 h. The CFUs on the plates of different groups were counted and compared.

https://doi.org/10.2147/JIR.S535747

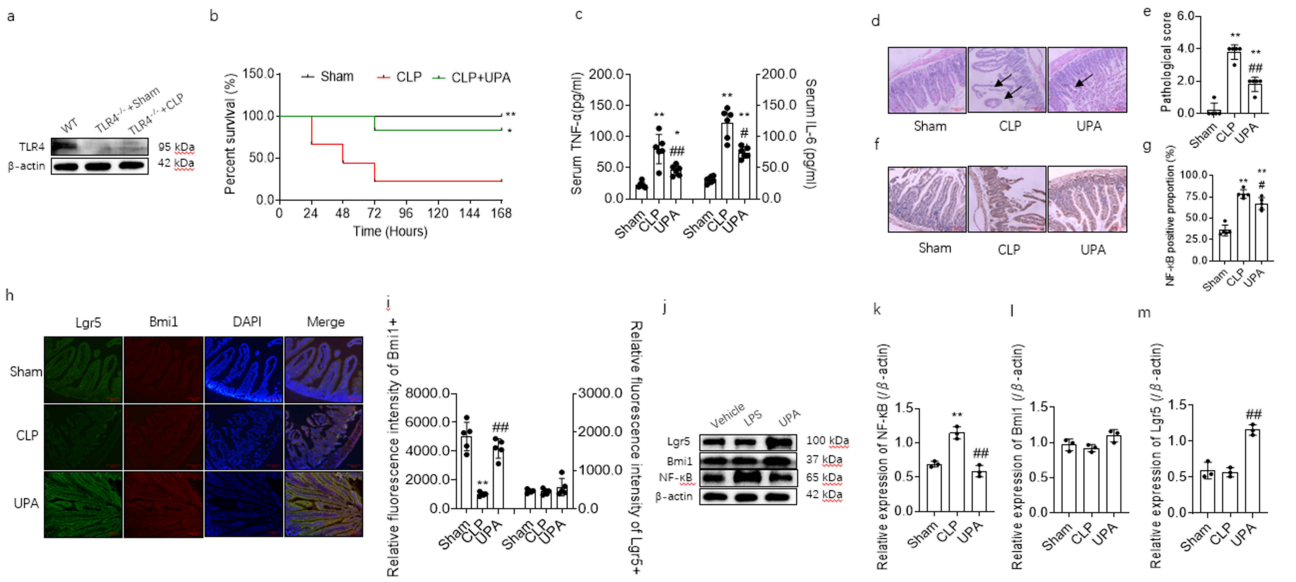

Figure 3 UPA protects CLP-induced sepsis TLR4$^{-/-}$ mice. (**a**) Western blotting assay of TLR4 protein in wild type mice and TLR4$^{-/-}$ mice; (**b**) Animal survival among groups (Kaplan-Meier). *$p < 0.05$, **$p < 0.01$ vs CLP; (**c**) Serum TNF-α and IL-6 assays of sepsis TLR4$^{-/-}$ mice ($\bar{x} \pm s$, n = 6). *$p < 0.05$, **$p < 0.01$ vs Sham, $^{\#}p < 0.05$, $^{\#\#}p < 0.01$ vs CLP. The peripheral blood was collected 6 h after the CLP surgeries. Next, the sera were isolated, and the serum TNF-α and IL-6 levels were detected by using ELISA kits in accordance with the instructions; (**d** and **e**) Pathology and score of small intestines of sepsis mice in groups ($\bar{x} \pm s$, n = 5) (Bar = 10 μm). **$p < 0.01$ vs Sham, $^{\#\#}p < 0.01$ vs CLP. The collected small intestines were fixed and then stained with H&E. The pathological examination was conducted described as before; (**f** and **g**) Immunohistochemistry assay of NF-κB protein in small intestines of sepsis mice in groups ($\bar{x} \pm s$, n = 5) (Bar = 10 μm). **$p < 0.01$ vs Sham. The embedded small intestine paraffins were dewaxed, hydrated, and stained as before; (**h** and **i**) Immunofluorescence staining assays of Bmi1 and Lgr5 in small intestines of sepsis mice (Bar = 10 μm). **$p < 0.01$ vs Sham, $^{\#\#}p < 0.01$ vs CLP; (**j–m**) Western blotting assays of NF-κB, Bmi1, and Lgr5 proteins in small intestines of TLR4$^{-/-}$ mice ($\bar{x} \pm s$, n = 3). **$p < 0.01$ vs Vehicle, $^{\#}p < 0.05$, $^{\#\#}p < 0.01$ vs CLP.

UPA Alleviates Intestinal Injuries of CLP-Treated TLR4$^{-/-}$ Mice

Compared with the sham, the CLP resulted in intestinal injuries including swollen epithelial cells, inflammatory cell infiltration, and irregular arrangement of the intestinal glands (shown by arrows). Basically, UPA significantly alleviated intestinal edema and inflammatory cell infiltration, which restored part intestinal epithelial integrity and normal structure (Figure 3d). In addition, UPA remarkably reduced pathological score of the intestines ($F = 81.33$, $p < 0.0001$) (Figure 3e).

UPA Reduces NF-κB Expression in Small Intestines of CLP-Treated TLR4$^{-/-}$ Mice

The immunohistochemistry showed that the CLP significantly increased the intestinal NF-κB expression compared to the sham. Compared with the CLP, UPA significantly decreased the intestinal NF-κB expression (Figure 3f and g) ($F = 63.86$, $p < 0.0001$).

UPA Increases Bmi1 Immunofluorescence in Intestines of CLP-Treated TLR4$^{-/-}$ Mice

In the TLR4$^{-/-}$ mice, the CLP markedly reduced the intestinal Bmi1 not Lgr5 expression compared to the sham. The intestinal Bmi1 not Lgr5 expression was significantly elevated in the UPA group than that in the CLP group (Bmi1: $F = 46.30$, $p < 0.0001$; Lgr5: $F = 1.078$, $p = 0.3711$). (Figure 3h and i).

UPA Reduces Intestinal NF-κB, and Increases Lgr5 Protein Expressions of CLP-Treated TLR4$^{-/-}$ Mice

There was a significant difference in intestinal Lgr5 expression between the sham group and the CLP group. UPA markedly reduced NF-κB ($F = 46.68$, $p = 0.0002$) and increased Lgr5 ($F = 43.56$, $p = 0.0003$). However, it had no significant influence on the Bmi1 expression compared to the CLP ($F = 4.395$, $p = 0.0668$) (Figure 3j–m).

Proteomics Analysis of Differential Proteins in LPS-Treated RAW264.7 Cells

The proteomics analysis showed that the distribution of normalized abundance values for all samples, and the box shape and violin shape between biological duplicate samples were relatively close (Figure 4a). In addition, the principal component analysis (PCA) showed that a good sample separation and a clear clustering for the samples among these three groups (Figure 4b).

In the RAW264.7 cells, there were a total of 69 upregulated and 119 downregulated differential proteins between the UPA-treated and LPS-treated (Figure 4c). Also, the Complex Heatmap showed that the significantly downregulated proteins were more in the UPA-treated group, and the significantly upregulated proteins were more in the LPS-treated group(Figure 4d).

After that, top eight inflammation-related differential proteins (UPA vs LPS) including seven downregulated and one upregulated were selected for analysis. Compared with LPS, UPA significantly downregulated interferon-activable protein (IAP) 203 (t = 13.71, $p = 0.0053$), IAP 204 (t = 29.24, $p = 0.0012$), IAP 207 (t = 35.14, $p = 0.0008$), 2′-5′-oligoadenylate synthase 2 (t = 21.47, $p = 0.0022$), STAT2 (t = 157.2, $p < 0.0001$), TNF-α (t = 11.09, $p = 0.0080$), IL-1β (t = 6.401, $p = 0.0235$), and markedly upregulated leukemia inhibitory factor (LIF) (t = 9.864, $p = 0.0101$) (Figure 4e–l).

Go and KEGG Analysis

The gene ontology (Go) functional annotations showed that major of the differential proteins were involved in biological process (BP) and molecular function (MF), and only a few were in cellular component (CC) (Figure 5a). Respectively, the upregulated and downregulated differential proteins in each annotation were labelled with orange and blue colors (Figure 5b).

The KEGG analysis showed that the differential pathways participated in human diseases, organismal systems, environmental information processing and others (Figure 5c). Moreover, NOD-like receptor (NLR) signaling pathway was most significantly affected between the LPS-treated and UPA-treated. Therefore, some key members in this pathway such as NLRP3 and IL-1β proteins were preliminarily measured by Western blotting.

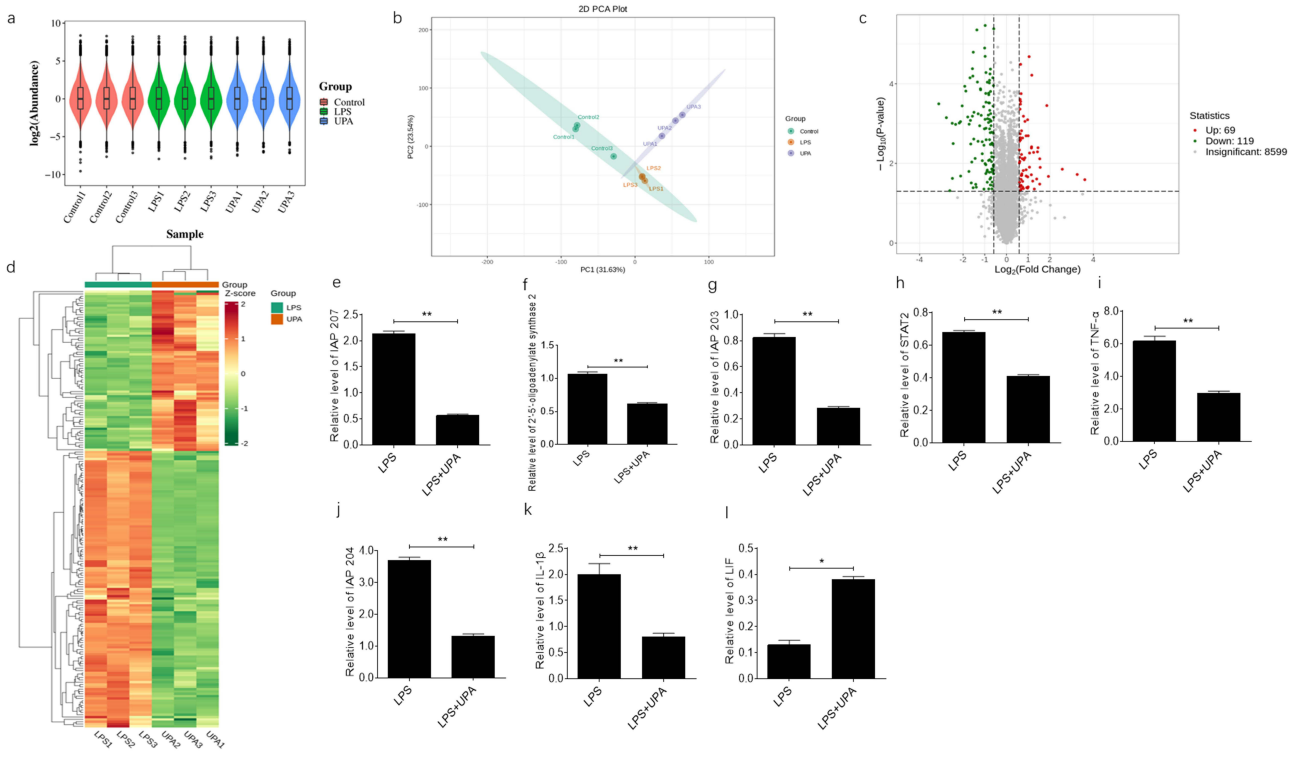

Figure 4 Proteomics analysis of UPA inhibiting LPS-induced inflammation in RAW264.7 cells. (**a**) Violin plot of distribution of all samples; (**b**) PCA assay of showed separation and clustering for the samples; (**c**) Volcano plot of differential expressed proteins between UPA-treated and LPS-treated in the RAW264.7 cells; (**d**) Complex heatmap for upregulated and downregulated proteins between UPA-treated and LPS-treated; (**e–l**) top 8 inflammation-related differential proteins ($\bar{x} \pm s$, n = 3). *$p < 0.05$, **$p < 0.01$ vs LPS.

https://doi.org/10.2147/JIR.S535747

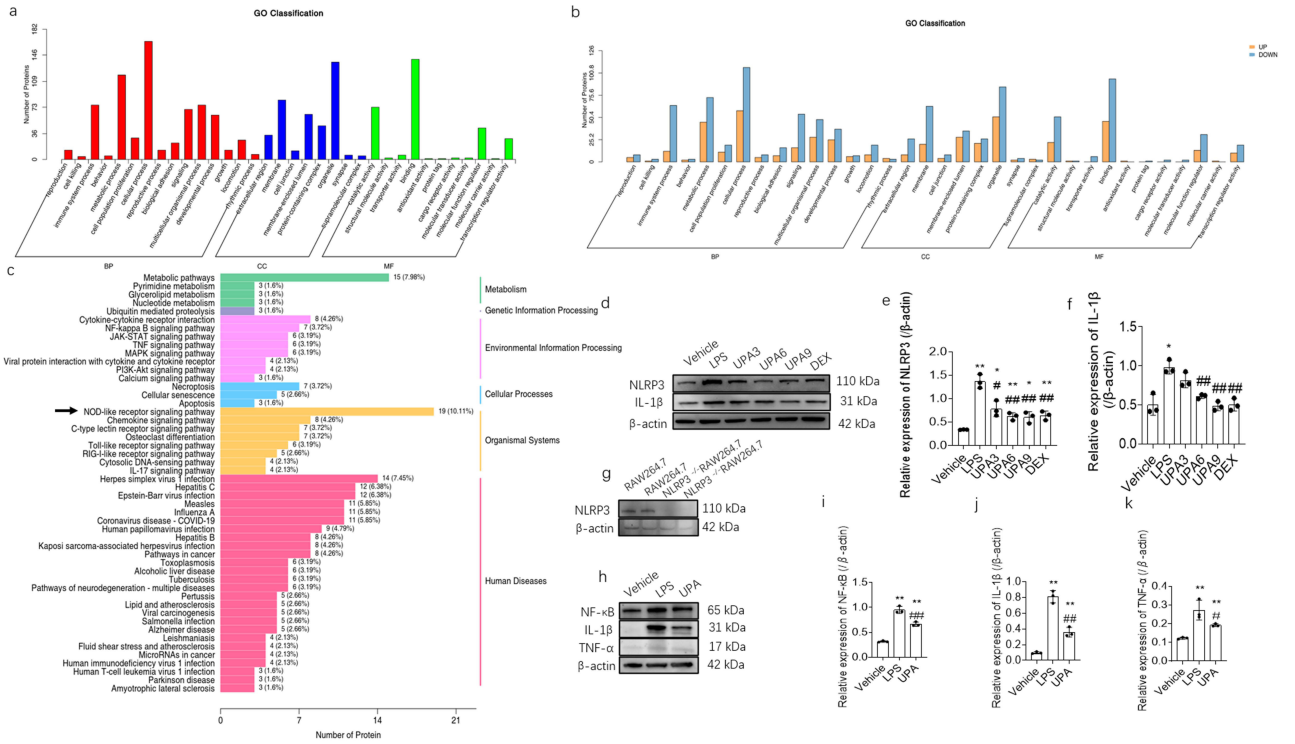

Figure 5 UPA inhibits LPS-induced inflammation in RAW264.7 cells independent of NLRP3 pathway. (**a**) Go analysis of major of differential proteins between UPA-treated and LPS-treated in different annotations; (**b**) Go analysis of upregulated proteins and downregulated proteins between UPA-treated and LPS-treated in each annotation; (**c**) KEGG analysis of differential pathways between UPA-treated and LPS-treated; (**d–f**) Western blotting assays of NLRP3 and IL-1β proteins in the RAW264.7 cells after treatments ($\bar{x} \pm s$, n = 3). $^{*}p < 0.05$, $^{**}p < 0.01$ vs Vehicle; $^{\#}p < 0.05$, $^{\#\#}p < 0.01$ vs LPS; (**g**) Western blotting assay of NLRP3 protein in RAW264.7 cells and NLRP3$^{-/-}$ RAW264.7 cells; (**h–k**) UPA reduces NF-κB, TNF-α, and IL-1β protein expressions in LPS-treated NLRP3$^{-/-}$ RAW264.7 cells ($\bar{x} \pm s$, n = 3). $^{*}p < 0.05$, $^{**}p < 0.01$ vs Vehicle, $^{\#}p < 0.05$, $^{\#\#}p < 0.01$ vs LPS. Respectively, the cells were treated with vehicle, LPS, and LPS plus UPA. Four hours post the treatments, the precipitates were collected for Western blotting assays of NF-κB, TNF-α, and IL-1β proteins.

Western Blotting Assay in RAW264.7 Cell Line and Experiment Validation in NLRP3$^{-/-}$ RAW264.7 Cell Line

Compared with the vehicle, the LPS significantly upregulated NLRP3 and IL-1β protein expressions in the RAW264.7 cells. While, UPA significantly downregulated the increased expressions of these two NLR-related proteins compared to LPS (NLRP3: F = 27.11, $p < 0.0001$; IL-1β: F = 17.06, $p < 0.0001$) (Figure 5d–f).

Further, the role of NLRP3 was investigated to explore its anti-inflammatory role in vitro. Before the validation, the NLRP3 protein in the NLRP3$^{-/-}$ RAW264.7 cells was detected by Western blotting. It showed that almost no NLRP3 was expressed in this gene knockout cell line compared to the wild type cell line RAW264.7 (Figure 5g).

The LPS significantly upregulated the NF-κB, IL-1β, and TNF-α expressions in the gene knockout cell line. Compared with the LPS, UPA treatment significantly reduced the increased protein expressions of NF-κB (F = 128.2, $p < 0.0001$), IL-1β (F = 116.9, $p < 0.0001$), and TNF-α (F = 17.65, $p = 0.0031$) in the LPS-treated NLRP3$^{-/-}$ RAW264.7 cell line, which was some consistent with the Western blotting in the TLR4$^{-/-}$ RAW264.7 cell line (Figure 5h–k).

Discussion

Recently, a study has shown that tofacitinib and baricitinib significantly ameliorates sepsis-induced cognitive function damage in mice. Further, these two JAK inhibitors decrease neuroinflammation, oxidative stress, and neuronal damage.[21] In addition, baricitinib protects kidney injury in a CLP-induced sepsis rat model by reducing inflammation and apoptosis in a dose-dependent manner.[22]

JAK/STAT signaling pathway regulates macrophage polarization to reduce excessive inflammatory response.[14,15] Previously, a study revealed that TNF-α treatment recruited STAT-1α to the TNFR1, while IFN-ν exposure inhibited this association in the RAW264.7 cells. Reversely, in STAT-1α$^{-/-}$ cells TNF-α treatment induced a stronger activation of NF-

κB.[23] It suggested that STAT-1α availability was limited by IFN-ν via depleting STAT-1α. Alternatively, targeting this pathway is beneficial to treat sepsis and its complications.[24,25] In addition, a meta-analysis showed that neutropenia was a significant adverse reaction after long term application of UPA in treatment of patients with ankylosing spondylitis.[26]

The present study found that UPA significantly inhibited NF-κB, and its downstream proinflammatory cytokines such as TNF-α, IL-6, and IL-1β in the RAW264.7 cells. Similarly, UPA reduced NF-κB in the isolated macrophages and the intestines, and the inflammatory mediators in the isolated macrophages of the CLP-treated mice. Thus, NF-κB is a key molecule participating in the anti-inflammatory event of UPA.

NF-κB plays a crucial role to initiate inflammatory responses. Usually, the inhibitor of NF-κB (IκB) binds to NF-κB to prevent it from entering the nucleus and exerting transcriptional effects. The phosphorylation of iκB plays a crucial role in inflammatory and immune responses. Its excessive phosphorylation may lead to excessive immune response and trigger autoimmune diseases. Our findings demonstrated that the LPS treatment for 4 h increased NF-κB and p-iκBα in the RAW264.7 cells, which was some consistent with a previous study that LPS increased the phosphorylation of IkBα in Tim-3-CD4 T cells.[27] In the present study, UPA significantly reduced NF-κB and p-iκBα expressions not only in the LPS-treated RAW264.7 cells but also in the CLP-treated macrophages isolated from PLFs. Further, the inhibition of NF-κB and p-iκB was beneficial to reduce the downstream cytokines such as TNF-α and IL-6.[28]

In addition, our study showed that UPA significantly reduced bacterial loads in PLFs of a CLP-induced sepsis mouse model. Up to now, no studies have reported the antibacterial effect of UPA. We speculated UPA treatment might enhance bacterial phagocytosis of macrophages or organs,[29,30] thereby reducing bacterial overgrowth-related translocation, which was linked to the decreased expressions of some inflammatory mediators such as TH1/TH2/TH17 cytokines.[31] It needs investigations in the further studies.

It has revealed that Bmi1 prevents aging to maintain intestinal tight junctions, epithelial barrier function, and microbial balance.[32] In addition, the self-renewal and high differentiation potential of Lgr5+ ISCs plays an important role for repairing intestinal mucosal injury.[33] Currently, it has been confirmed that Bmi1 and Lgr5 are decreased in intestinal epithelial cells after the LPS treatment.[34,35]

Our study showed decreased Bmi1 and Lgr5 expressions in intestines under CLP-induced sepsis status. Further, high-dose UPA and DEX significantly reduced the bacterial load, and CLP-induced inflammation-related mediators. Therefore, UPA and DEX upregulated the intestinal Bmi1 and Lgr5 expressions, thereby maintaining the integrity of intestinal epithelial mucosa barrier, which reduced bacterial translocation into the abdominal cavity.

To further explore the role of TLR4/NF-κB pathway, we selected $TLR4^{-/-}$ RAW264.7 cell line and $TLR4^{-/-}$ mice to validate the mechanism of UPA. However, the findings suggested that UPA still exerts its anti-inflammatory effect in vitro and in vivo when the TLR4 gene was knock-out. So, the TLR4/NF-κB pathway was not the main target pathway of UPA. Alternatively, UPA exerted its anti-inflammatory effect in vitro and in vivo independent of the TLR4/NF-κB pathway.

Comparative proteomics was used to screen the differential inflammation-related proteins to investigate the in vitro anti-inflammatory mechanism of UPA more accurately. It showed that NLR signaling pathway was most significantly affected between the UPA-treated and the LPS-treated.

A study reveals that NLRP3 inflammasome is involved in various inflammation related diseases and may be a key regulatory factor in occurrence and development of inflammatory diseases.[36] During hemorrhagic shock, high mobility protein 1 can activate lung endothelial cell NAD(P)H oxidase through the TLR4 mode to generate ROS, thereby dissociating those proteins interacting with thioredoxin, which induces NLRP3 inflammasome activation and IL-1β secretion.[37] Thus, inhibition of NLRP3 might be a potential target to improve inflammatory responses in related diseases. UPA significantly reduced the protein expressions of NLRP3 and IL-1β compared to the LPS treatment in the RAW264.7 cells, suggesting possible participation of the NLRP3 pathway in anti-inflammatory effect of UPA in vitro.

To deeply clarify the role of NLRP3 in the in vitro anti-inflammatory effect of UPA, the $NLRP3^{-/-}$ RAW 264.7 cells were used to validate the mechanism. However, the anti-inflammatory effect of this compound was not significantly abolished, including still decreased NF-κB, TNF-α, and IL-1β expressions in this gene knockout cell line after UPA treatment. Thus, the NLRP3 is not the main target of UPA inhibiting LPS-induced inflammation, which is some inconsistent with the proteomics analysis.

Study Limitations

The present study has some limitations including (i) limitation of long-term UPA exposure for animal models; (ii) limitation in capturing sex-based immune differences for only use of male animals; (iii) lack of infection model diversity for only use of a CLP model.

Future Directions

i. Evaluation of UPA in combination with antibiotics or supportive therapies;
ii. Investigations of UPA in larger animal models or human ex vivo tissues;
iii. Broader pathway screening via transcriptomics or phosphoproteomics.

Conclusions

In summary, UPA reduces the LPS- and CLP-induced inflammatory responses in vitro and in vivo by inhibiting NF-κB and its downstream cytokines. This study will provide a promising medication to treat sepsis and its related complication such as intestinal injury. The mechanism of UPA against sepsis needs further investigations.

Abbreviations

ANOVA, One-way analysis of variance; BCA, Bicinchoninic acid assay; BSA, Bovine serum albumin; CLP, Cecal ligation and puncture; DAPI, 4′,6-diamidino-2-phenylindole; DEX, Dexamethasone; ECL, Enhanced chemiluminescence; H&E, Hematoxylin and eosin; HPLC, High performance liquid chromatography; IAP, Interferon-activable protein; ICR, Institute of cancer research; IFN, Interferon; IL, Interleukin; JAK, Janus kinase; LPS, Lipopolysaccharide; MODS, Multiple organ dysfunction syndrome; NF-κB, Nuclear factor kappa-B; NIH, National institutes of health; NLR, NOD-like receptor; NLRP3, NOD-, LRR- and pyrin domain-containing protein 3; RT-PCR, Reverse transcription-polymerase chain reaction; SIRS, Systemic inflammatory response syndrome; SPF, Specific pathogen free; STAT, Signal transducer and activator of transcription; TLR, Toll-like receptor; TNF, Tumor necrosis factor; TNFR, Tumor necrosis factor receptor; UPA, Upadacitinib.

Data Sharing Statement

The data in this study are deposited in the figshare repository, and the accession number is 10.6084/m9.figshare.29818952.

Acknowledgments

The authors would like to thank Fengzi Biotechnology Co., Ltd (Nanjing, China) for its technical support in the proteomics assay.

Funding

This work was supported by grants from 2022 High-Level Talent Research Project of Yunnan Provincial Health Commission (2023-KHRCBZ-A02), and Open Projects for Construction Unit of Clinical Pharmacy Center of Yunnan Province (2023YJZX-YX11).

Disclosure

The authors declared no conflicts of interest in this study.

References

1. Gobatto AL, Besen BA, Azevedo LC. How can we estimate sepsis incidence and mortality? *Shock*. 2017;47:6–11. doi:10.1097/SHK.0000000000000703
2. Wang L, Lin F, Ren M, et al. The PICK1/TLR4 complex on microglia is involved in the regulation of LPS-induced sepsis-associated encephalopathy. *Int Immunopharmacol*. 2021;100:108116. doi:10.1016/j.intimp.2021.108116

3. Behairy MY, Abdelrahman AA, Toraih EA, et al. Investigation of TLR2 and TLR4 polymorphisms and sepsis susceptibility: computational and experimental approaches. *Int J Mol Sci*. 2022;23(18):10982. doi:10.3390/ijms231810982
4. Chen SN, Tan Y, Xiao XC, et al. Deletion of TLR4 attenuates lipopolysaccharide-induced acute liver injury by inhibiting inflammation and apoptosis. *Acta Pharmacol Sin*. 2021;42:1610–1619. doi:10.1038/s41401-020-00597-x
5. Kumar V. Toll-like receptors in sepsis-associated cytokine storm and their endogenous negative regulators as future immunomodulatory targets. *Int Immunopharmacol*. 2020;89:107087. doi:10.1016/j.intimp.2020.107087
6. Senousy SR, Ahmed AF, Abdelhafeez DA, Khalifa MMA, Abourehab MAS, El-Daly M. Alpha-chymotrypsin protects against acute lung, kidney, and liver injuries and increases survival in CLP-induced sepsis in rats through inhibition of TLR4/NF-κB pathway. *Drug Des Devel Ther*. 2022;16:3023–3039. doi:10.2147/DDDT.S370460
7. Xia YM, Guan YQ, Liang JF, Wu WD. TAK-242 improves sepsis-associated acute kidney injury in rats by inhibiting the TLR4/NF-kappaB signaling pathway. *Ren Fail*. 2024;46:2313176. doi:10.1080/0886022X.2024.2313176
8. Wang D, Jiang W, Zhu F, Mao X, Agrawal S. Modulation of the tumor microenvironment by intratumoral administration of IMO-2125, a novel TLR9 agonist, for cancer immunotherapy. *Int J Oncol*. 2018;53:1193–1203. doi:10.3892/ijo.2018.4456
9. Avunje S, Jung SJ. Poly (I:C) and imiquimod induced immune responses and their effects on the survival of olive flounder (Paralichthys olivaceus) from viral haemorrhagic septicaemia. *Fish Shellfish Immunol*. 2017;71:338–345. doi:10.1016/j.fsi.2017.10.032
10. Blauvelt A, Teixeira HD, Simpson EL, et al. Efficacy and safety of upadacitinib vs dupilumab in adults with moderate-to-severe atopic dermatitis: a Randomized clinical trial. *JAMA Dermatol*. 2021;157:1047–1055. doi:10.1001/jamadermatol.2021.3023
11. Smolen JS, Pangan AL, Emery P, et al. SELECT-MONOTHERAPY): a randomised, placebo-controlled, double-blind Phase 3 study. *Lancet*. 2019;393:2303–2311. doi:10.1016/S0140-6736(19)30419-2
12. McInnes IB, Anderson JK, Magrey M, et al. Trial of upadacitinib and adalimumab for psoriatic arthritis. *N Engl J Med*. 2021;384:1227–1239. doi:10.1056/NEJMoa2022516
13. Danese S, Vermeire S, Zhou W, et al. Upadacitinib as induction and maintenance therapy for moderately to severely active ulcerative colitis: results from three phase 3, multicentre, double-blind, randomised trials. *Lancet*. 2022;399:2113–2128. doi:10.1016/S0140-6736(22)00581-5
14. Xiong W, Zhan Y, Xiao R, Liu F. Advancing sepsis diagnosis and immunotherapy machine learning-driven identification of stable molecular biomarkers and therapeutic targets. *Sci Rep*. 2025;15:8333. doi:10.1038/s41598-025-93010-8
15. Purohit M, Gupta G, Afzal O, et al. Janus kinase/signal transducers and activator of transcription (JAK/STAT) and its role in Lung inflammatory disease. *Chem Biol Interact*. 2023;371:110334. doi:10.1016/j.cbi.2023.110334
16. Zhang X, Wang X, Sun L, Gao G, Li Y. Tofacitinib reduces acute lung injury and improves survival in a rat model of sepsis by inhibiting the JAK-STAT/NF-κB pathway. *J Inflamm*. 2023;20:5. doi:10.1186/s12950-023-00332-3
17. Yu J, Shen Y, Luo J, et al. Upadacitinib inhibits corneal inflammation and neovascularization by suppressing M1 macrophage infiltration in the corneal alkali burn model. *Int Immunopharmacol*. 2023;116:109680. doi:10.1016/j.intimp.2023.109680
18. Mitchell DC, Kuljanin M, Li J, et al. A proteome-wide atlas of drug mechanism of action. *Nat Biotechnol*. 2023;41:845–857. doi:10.1038/s41587-022-01539-0
19. Jia W, Wu X. Potential biomarkers analysis and protein internal mechanisms by cold plasma treatment: is proteomics effective to elucidate protein-protein interaction network and biochemical pathway? *Food Chem*. 2023;426:136664. doi:10.1016/j.foodchem.2023.136664
20. Jiang Y, Zhang C, Wang T. bFGF ameliorates intestinal mucosal permeability and barrier function through tight junction proteins in burn injury rats. *Burns*. 2021;47:1129–1136. doi:10.1016/j.burns.2020.11.004
21. Bhadauriya MS, Singh H, Suri M, Hanifa M, Bali A. JAK/STAT inhibitors mitigate sepsis-associated cerebral and cognitive injury. *Fundam Clin Pharmacol*. 2025;39:e70005. doi:10.1111/fcp.70005
22. Çakır M, Tarakçı B, Aydın A, Bircan B, Fırat S, Şekerci G. JAK1/JAK2 inhibitor baricitinib ameliorates sepsis-induced acute kidney injury in rats. *Eur J Pharmacol*. 2025;1002:177770. doi:10.1016/j.ejphar.2025.177770
23. Wesemann DR, Benveniste EN. STAT-1 alpha and IFN-gamma as modulators of TNF-alpha signaling in macrophages: regulation and functional implications of the TNF receptor 1: STAT-1 alpha complex. *J Immunol*. 2003;171:5313–5319. doi:10.4049/jimmunol.171.10.5313
24. Zhang H, Meng F, Tang J, et al. Lactate inhibits T-cell activation in sepsis through CD40LG downregulation and SOCS3-mediated JAK1/STAT3 pathway suppression. *Biochim Biophys Acta Mol Basis Dis*. 2025;1871:167923. doi:10.1016/j.bbadis.2025.167923
25. Li D, Weng Y, Wang G, Zhen G. Anti-septic potential of 7-alpha-Obacunyl acetate isolated from the toona sinensis on cecal ligation/puncture mice via suppression of JAK-STAT/NF-kappaB signal pathway. *Infect Drug Resist*. 2021;14:1813–1821. doi:10.2147/IDR.S302853
26. Yao Q, Zhu Y, Ma Y, Pu Y, Yang X, Zhang Z. Efficacy and safety of upadacitinib, a selective JAK-1 inhibitor in treatment of ankylosing spondylitis: a meta-analysis. *BMC Rheumatol*. 2025;9:19. doi:10.1186/s41927-025-00467-1
27. Huang S, Liu D, Sun J, et al. Tim-3 regulates sepsis-induced immunosuppression by inhibiting the NF-κB signaling pathway in CD4 T cells. *Mol Ther*. 2022;30:1227–1238. doi:10.1016/j.ymthe.2021.12.013
28. Wu Y, Wang Q, Li M, et al. SLAMF7 regulates the inflammatory response in macrophages during polymicrobial sepsis. *J Clin Invest*. 2023;133:e150224. doi:10.1172/JCI150224
29. Pugh ND, Jackson CR, Pasco DS. Total bacterial load within Echinacea purpurea, determined using a new PCR-based quantification method, is correlated with LPS levels and in vitro macrophage activity. *Planta Med*. 2013;79:9–14. doi:10.1055/s-0032-1328023
30. Ghosh B, Gaike AH, Pyasi K, et al. Bacterial load and defective monocyte-derived macrophage bacterial phagocytosis in biomass smoke-related COPD. *Eur Respir J*. 2019;53:1702273. doi:10.1183/13993003.02273-2017
31. Vega-Magaña N, Delgado-Rizo V, García-Benavides L, et al. Bacterial translocation is linked to increased intestinal IFN-γ, IL-4, IL-17, and mucin-2 in cholestatic rats. *Ann Hepatol*. 2018;17:318–329. doi:10.5604/01.3001.0010.8663
32. Athiyyah AF, Darma A, Ranuh R, et al. Lactobacillus plantarum IS-10506 activates intestinal stem cells in a rodent model. *Benef Microbes*. 2018;9:755–760. doi:10.3920/BM2017.0118
33. Ou W, Xu W, Wang Y, et al. Cooperation of Wnt/beta-catenin and Dll1-mediated Notch pathway in Lgr5-positive intestinal stem cells regulates the mucosal injury and repair in DSS-induced colitis mice model. *Gastroenterol Rep*. 2024;12:goae090. doi:10.1093/gastro/goae090
34. Yan KS, Chia LA, Li X, et al. The intestinal stem cell markers Bmi1 and Lgr5 identify two functionally distinct populations. *Proc Natl Acad Sci U S A*. 2012;109:466–471. doi:10.1073/pnas.1118857109

35. Zheng L, Duan SL, Wen XL, Dai YC. Molecular regulation after mucosal injury and regeneration in ulcerative colitis. *Front Mol Biosci*. 2022;9:996057. doi:10.3389/fmolb.2022.996057
36. Dhar R, Rana MN, Zhang L, et al. Phosphodiesterase 4B is required for NLRP3 inflammasome activation by positive feedback with Nrf2 in the early phase of LPS- induced acute lung injury. *Free Radic Biol Med*. 2021;176:378–391. doi:10.1016/j.freeradbiomed.2021.10.007
37. Xiang M, Shi X, Li Y, et al. Hemorrhagic shock activation of NLRP3 inflammasome in lung endothelial cells. *J Immunol*. 2011;187:4809–4817. doi:10.4049/jimmunol.1102093